Pasta phases in hot and dense matter

Hong Shen *Nankai University, Tianjin, China*

申虹 南開大学 天津 中国

Collaborators:

Jinniu Hu, Fan Ji,
Shishao Bao,
Xuhao Wu, Min Ju,
H. Toki,
K. Sumiyoshi,
K. Oyamatsu

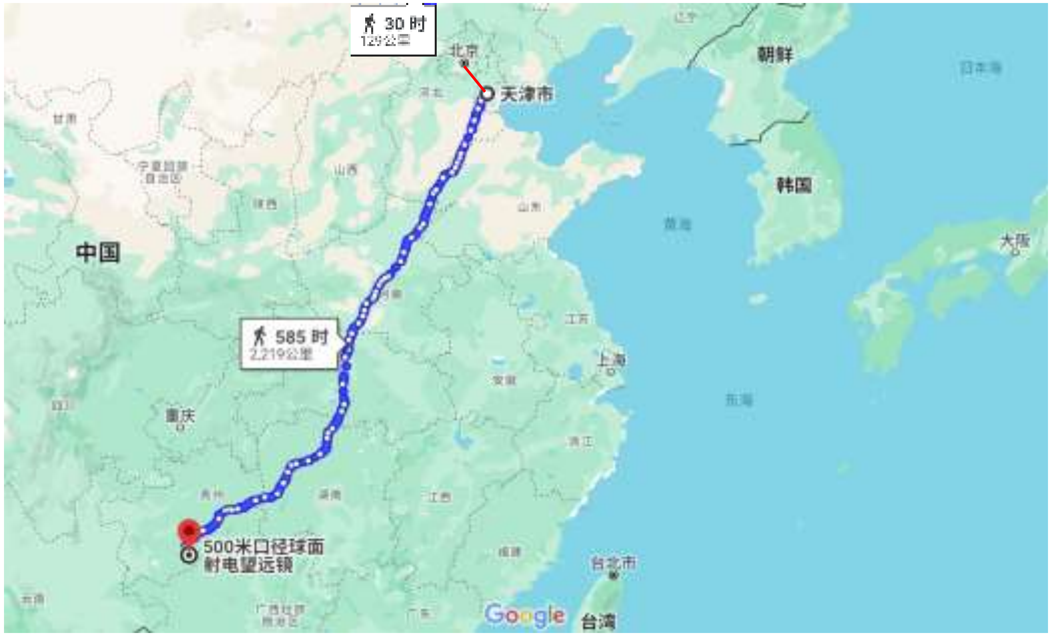

Introduction

"Physics is an experimental science"

物理学是一门实验科学

New physics is driven by observation and experiment

Introduction

nuclear physics

astrophysics

Equation of State **(EOS)**

- unstable nuclei
- nuclear reactions
- nucleosynthesis
- ......

- supernova explosion
- proton-neutron star cooling
- neutron star properties
- binary mergers
- ......

Classification of EOS

EOS for supernovae

temperature (T):

0 ~ 100 MeV

proton fraction (Yp):

0 ~ 0.6

construction:

nonuniform + uniform

EOS for neutron stars

temperature (T):

T = 0

proton fraction (Yp):

β equilibrium

construction:

crusts + core

nuclear pasta

Phase diagram

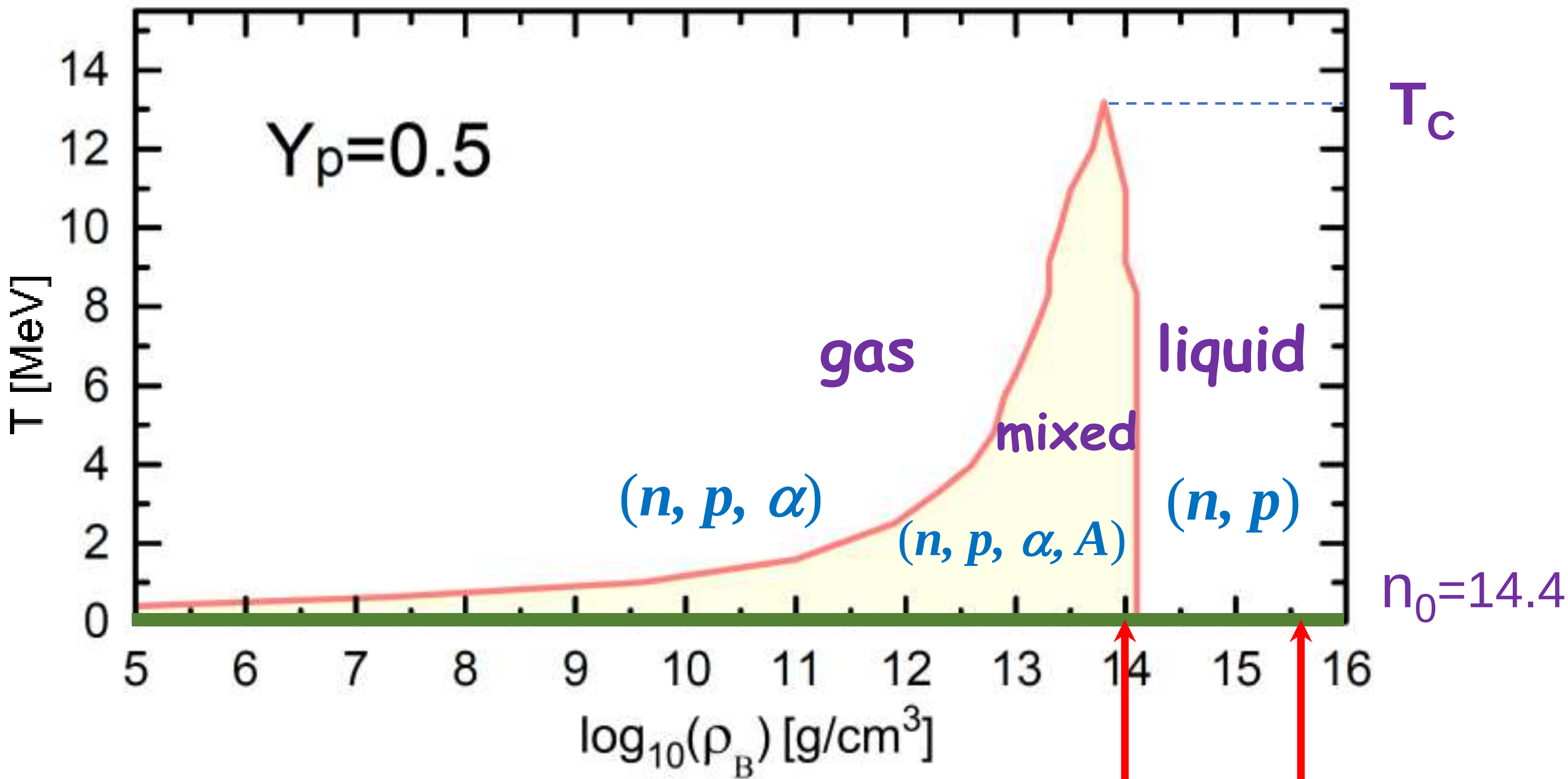

T~0, β equilibrium

crust-core phase transition

nuclear liquid-gas phase transition

gas: + other light clusters

mixed: nonuniform, + pasta

liquid: + hyperons, + quarks

CompOSE https://compose.obspm.fr

- Home
- EoS
  - All families
  - Cold Neutron Star EoS
  - Cold Matter EoS
  - Neutron Matter EoS
  - General Purpose EoS
    - Models with hyperons and Delta-resonances
    - hybrid (quark-hadron) model
    - models with hyperons
    - Models with kaon condensate
    - nucleonic models
    - quark models
    - All
  - Neutron star crust EoS
- Bibliography
- Downloads
- Log In
- Newsletters
- External Links

CompOSE

CompStar Online Supernovae Equations of State

+	3	STOS(TM1L) with Lambda hyperons and electrons	General Purpose EoS	models with hyperons	Relativistic density functional models	SNA models	65	details
+	3	FYSS(TM1) (with electrons)	General Purpose EoS	nucleonic models	Relativistic density functional models	NSE models	65	details
+	3	FTNS(KOST2) variational EoS (no electrons)	General Purpose EoS	nucleonic models	Microscopic calculations	NSE models	65	details
+	3	SFHPST(TM1B145), with electrons	General Purpose EoS	hybrid (quark-hadron) model	Relativistic density functional models	SNA models	65	details
+	3	FTNS(KOST2) variational EoS (with electrons)	General Purpose EoS	nucleonic models	Microscopic calculations	NSE models	65	details
+	3	TNTYST(KOST2) variational EoS (with electrons)	General Purpose EoS	nucleonic models	Microscopic calculations	SNA models	65	details
+	3	SNSH(TM1e)	General Purpose EoS	nucleonic models	Relativistic density functional models	SNA models	65	details

Pasta phases

3D Thomas-Fermi calculations
of nuclear pasta phases at T=0

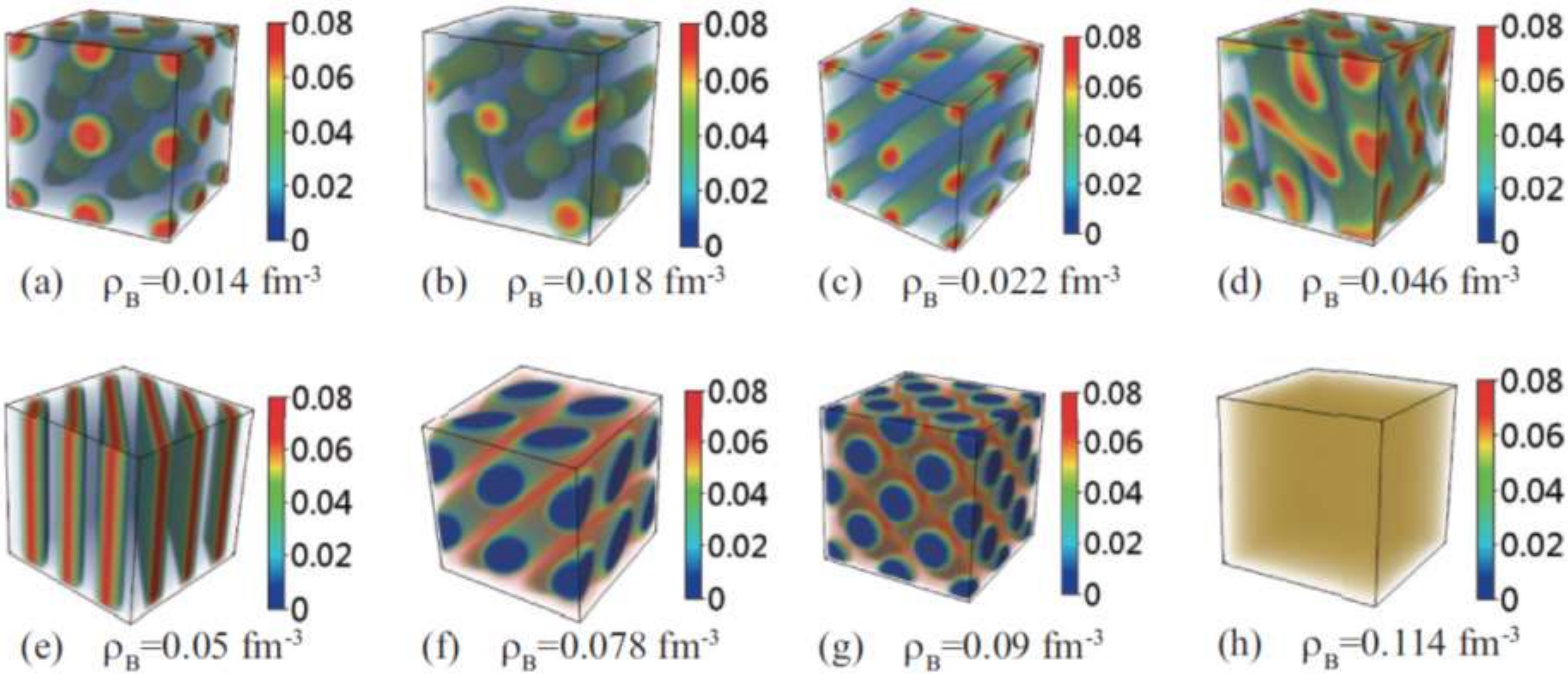

F. Ji, J. N. Hu, H. Shen, PRC 103, 055802 (2021)

Pasta phases with liquid-drop model

Progress of Theoretical Physics, Vol. 71, No. 2, February 1984

Shape of Nuclei in the Crust of Neutron Star

Masa-aki HASHIMOTO, Hironori SEKI and Masami YAMADA*

Department of Physics and Applied Physics, Waseda University, Tokyo 160
**Science and Engineering Research Laboratory, Waseda University, Tokyo 160*

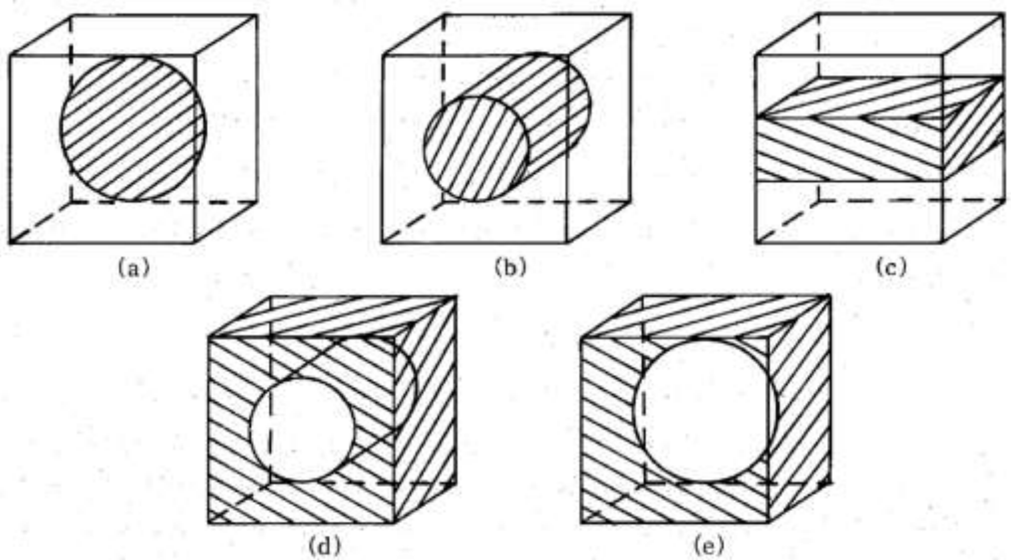

"the stable nuclear shape is likely to change successively from sphere to cylinder, board, cylindrical hole and spherical hole before uniform neutron-star matter is formed."

Pasta phases with Thomas-Fermi approximation

PHYSICAL REVIEW C **88**, 025801 (2013)

Nuclear "pasta" structures in low-density nuclear matter and properties of the neutron-star crust

Minoru Okamoto,[1,2] Toshiki Maruyama,[2] Kazuhiro Yabana,[1,3] and Toshitaka Tatsumi[4]

3D calculations using the RMF model under Thomas-Fermi approximation at T=0

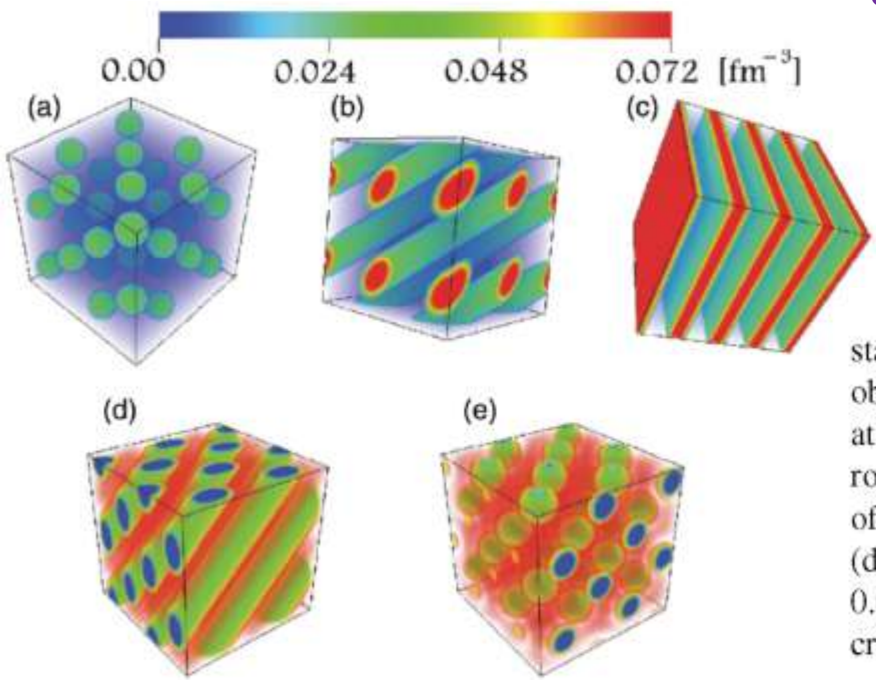

FIG. 1. (Color online) Proton density distributions in the ground states of symmetric matter ($Y_p = 0.5$). Typical pasta phases are observed: (a) Spherical droplets with an fcc crystalline configuration at baryon density $\rho_B = 0.01$ fm^{-3}, of 98 fm each side. (b) Cylindrical rods with a honeycomb crystalline configuration at 0.024 fm^{-3}, of 76 fm each side. (c) Slabs at 0.05 fm^{-3}, of 95 fm each side. (d) Cylindrical tubes with a honeycomb crystalline configuration at 0.08 fm^{-3}, of 79 fm each side. (e) Spherical bubbles with an fcc crystalline configuration at 0.09 fm^{-3}, of 97 fm each side.

Pasta phases with Quantum Molecular Dynamics

Phases of hot nuclear matter at subnuclear densities

G.Watanabe, K.Sato, K.Yasuoka, T.Ebisuzaki, PRC 69, 055805 (2004)

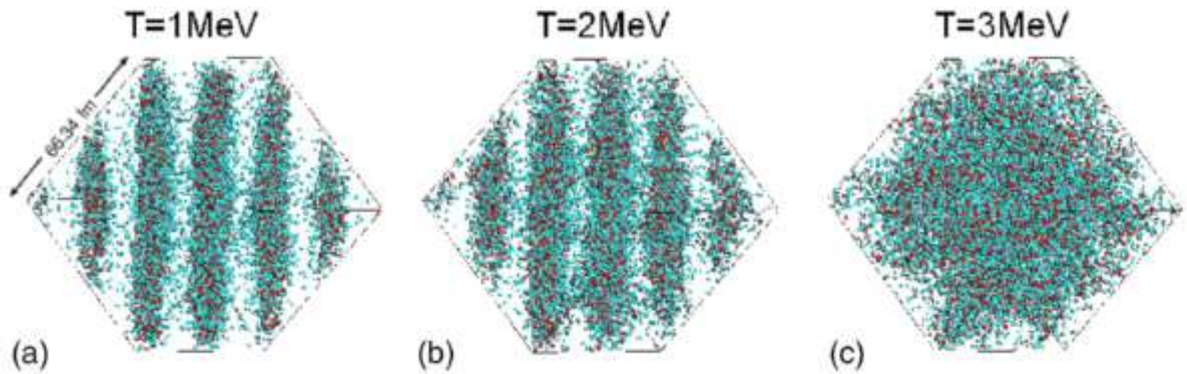

FIG. 9. (Color online) The nucleon distributions for $x=0.3$, $\rho=0.34\rho_0$ at the temperatures of 1, 2, and 3 MeV. 16384 nucleons are contained in the simulation box of size $L_{box}=66.34$ fm. Protons are represented by the red particles, and neutrons by the green ones. These figures are shown in the direction parallel to the plane of the slablike nuclei at $T=0$.

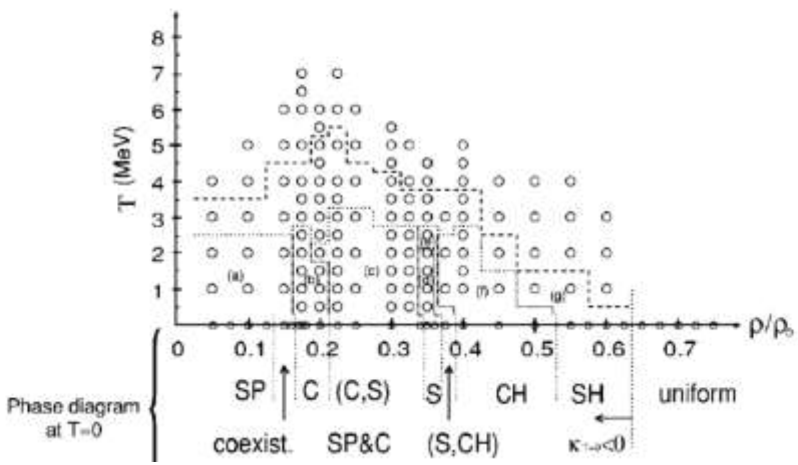

FIG. 19. Phase diagram of matter at $x=0.3$ plotted in the ρ-T plane.

Pasta phases with Skyrme-Hartree-Fock + BCS

Nuclear Pasta Phase in Core-Collapse Supernova Matter

H. Pais and J. R. Stone, PRL 109, 151101 (2012)

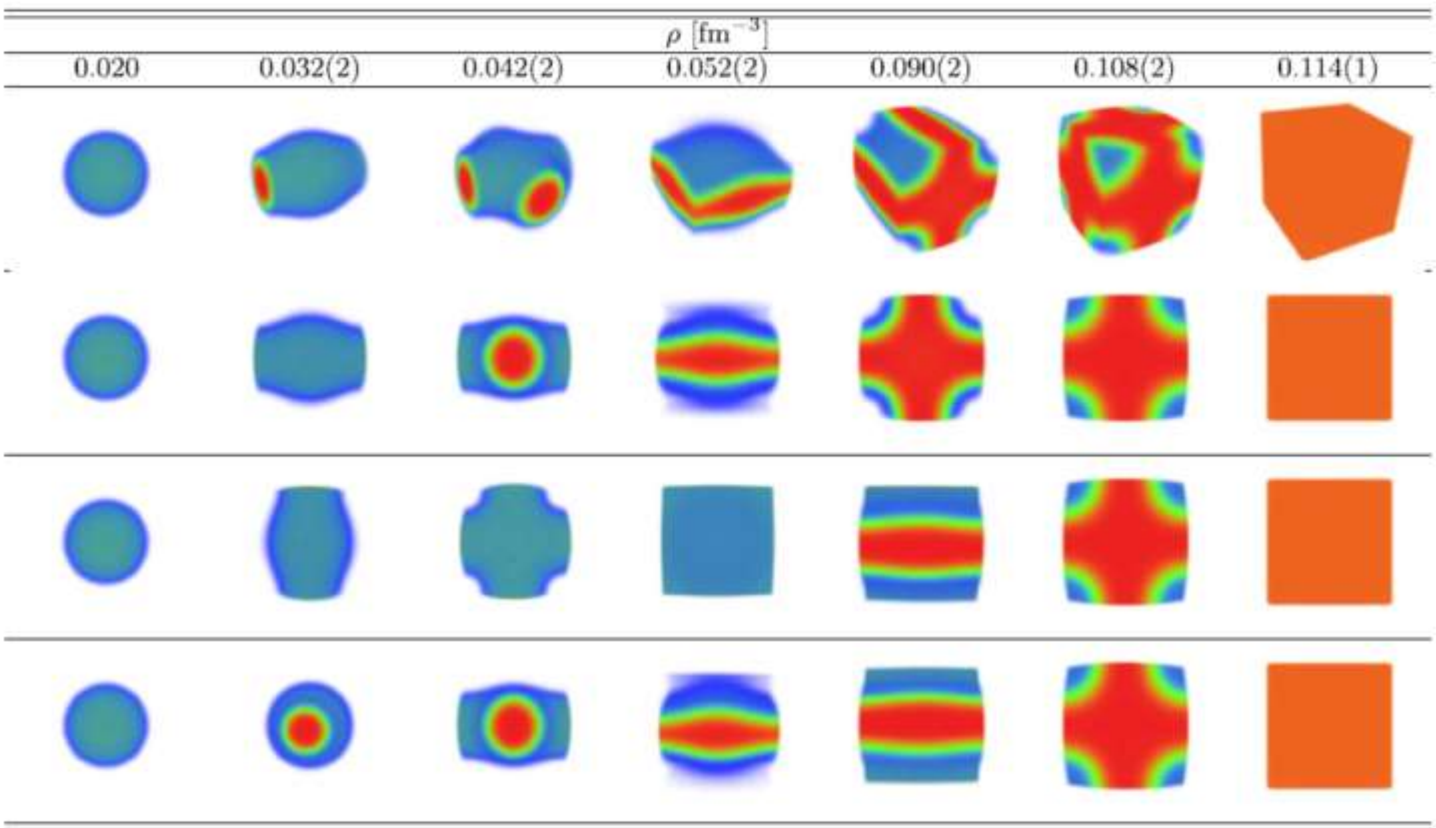

FIG. 1 (color online). First row: Pasta phases calculated using the SQMC700 Skyrme interaction, T=2 MeV and Yp=0.3. Rows 2, 3, 4: 2D projection of the pasta phases on the (y, x), (x, z), and (y, z) planes, respectively.

Effect of pasta phases on EOS

What is the effects of pasta phases on the realistic EOS?

	Shen EOS4	pasta phase
reference:	ApJ 891 (2020) 148	PRC 102 (2020) 015806
nuclear model:	RMF (TM1e)	RMF (TM1e + TM1)
method:	parametrized Thomas-Fermi	compressible liquid-drop
constituents:	n, p, α, A (spherical)	n, p, α, A (pasta)
results:	phase diagram E, P, S, ...	phase diagram E, P, S, ...

Relativistic Mean Field (RMF)

* extended TM1 model with different L by turning g_ρ and Λ_v

$$
\begin{aligned}
\mathcal{L}_{\rm RMF} = & \bar{\psi}\left[i\gamma_\mu\partial^\mu-(M+g_\sigma\sigma)-\left(g_\omega\omega^\mu+\frac{g_\rho}{2}\tau_a\rho^{a\mu}\right)\gamma_\mu\right]\psi \\
& +\frac{1}{2}\partial_\mu\sigma\partial^\mu\sigma-\frac{1}{2}m_\sigma^2\sigma^2-\frac{1}{3}g_2\sigma^3-\frac{1}{4}g_3\sigma^4 \\
& -\frac{1}{4}W_{\mu\nu}W^{\mu\nu}+\frac{1}{2}m_\omega^2\omega_\mu\omega^\mu+\frac{1}{4}c_3\left(\omega_\mu\omega^\mu\right)^2 \\
& -\frac{1}{4}R_{\mu\nu}^aR^{a\mu\nu}+\frac{1}{2}m_\rho^2\rho_\mu^a\rho^{a\mu}+\Lambda_v\left(g_\omega^2\omega_\mu\omega^\mu\right)\left(g_\rho^2\rho_\mu^a\rho^{a\mu}\right)
\end{aligned}
$$

* TM1e and TM1 parameter sets (same isoscalar properties)

TABLE I. Coupling constants of the TM1e and TM1 models with symmetry energy E_{sym} and slope L at saturation density.

Model	E_{sym} (MeV)	L (MeV)	g_σ	g_ω	g_ρ	g_2 (fm^{-1})	g_3	c_3	Λ_v
TM1e	31.38	40	10.0289	12.6139	13.9714	−7.2325	0.6183	71.3075	0.0429
TM1	36.89	110.8	10.0289	12.6139	9.2644	−7.2325	0.6183	71.3075	0.0000

Symmetry energy

* energy per particle w as function of n and $\alpha = \dfrac{n_n - n_p}{n}$

$$w = w_0 + \frac{K_0}{18n_0^2}(n-n_0)^2 + \left[\underline{S_0 + \frac{L}{3n_0}(n-n_0)}\right]\alpha^2$$

symmetry energy slope $L = 3n_0 \left[\dfrac{\partial E_{\rm sym}(n_b)}{\partial n_b}\right]_{n_b=n_0}$

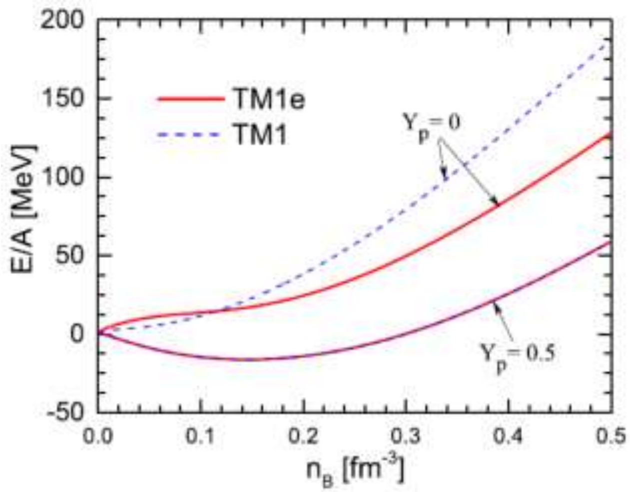

Figure 1. Energy per baryon E/A of symmetric nuclear matter and neutron matter as a function of the baryon number density n_B in the TM1e and TM1 models.

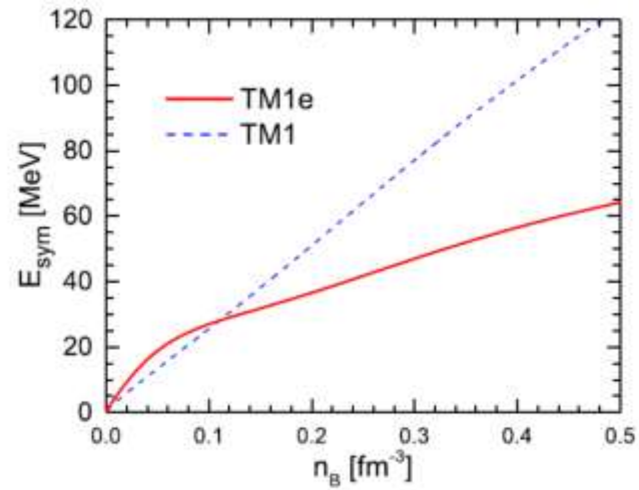

Figure 2. Symmetry energy E_{sym} as a function of the baryon number density n_B in the TM1e and TM1 models.

H. Shen, F. Ji, J. N. Hu, K.Sumiyoshi, ApJ 891, 148 (2020)

Method for pasta phases

*** compressible liquid-drop (CLD) model**

sharp interface

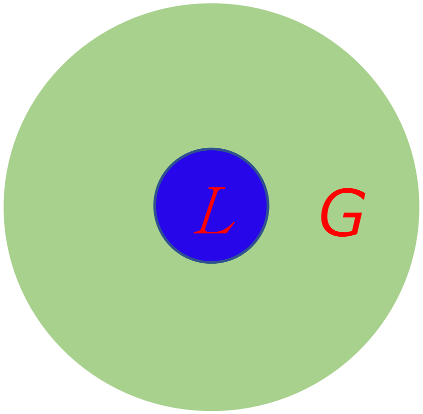

The equilibrium state can be determined by minimization of the total free energy density

$$f = u f^L(n_p^L, n_n^L) + (1-u) f^G(n_p^G, n_n^G, n_\alpha^G) + f_{\rm surf}(u, r_D, \tau) + f_{\rm Coul}(u, r_D, n_p^L, n_p^G, n_\alpha^G)$$

surface and Coulomb terms

$$f_{\rm surf} = \frac{D\tau u_{\rm in}}{r_D}$$

$$\Phi(u_{\rm in}) = \begin{cases} \frac{1}{D+2}\left(\frac{2 - D u_{\rm in}^{1-2/D}}{D-2} + u_{\rm in}\right), & D = 1, 3 \\ \frac{u_{\rm in} - 1 - \ln u_{\rm in}}{D+2}, & D = 2. \end{cases}$$

$$f_{\rm Coul} = \frac{e^2}{2}(\delta n_c)^2 r_D^2 u_{\rm in} \Phi(u_{\rm in})$$

Method for pasta phases

* **equilibrium conditions between L and G phases**

chemical potentials

$$\mu_n^G = \mu_n^L,$$

$$\mu_p^G = \mu_p^L + \frac{2 f_{\mathrm{Coul}}}{u(1-u)\delta n_c},$$

$$\mu_\alpha^G = 2\mu_p^G + 2\mu_n^G.$$

pressure

$$P^G = P^L + \frac{2 f_{\mathrm{Coul}}}{\delta n_c}\left(\frac{n_p^L}{u} + \frac{n_p^G + 2n_\alpha^G}{1-u}\right)$$

$$\mp \frac{f_{\mathrm{Coul}}}{u_{\mathrm{in}}}\left(3 + u_{\mathrm{in}}\frac{\Phi'}{\Phi}\right),$$

Method for pasta phases

* equilibrium between surface and Coulomb terms

$$f_{\rm surf} = 2 f_{\rm Coul}$$

$$r_D = \left[\frac{\tau D}{e^2 (\delta n_c)^2 \Phi} \right]^{1/3} \qquad r_C = u_{\rm in}^{-1/D} r_D$$

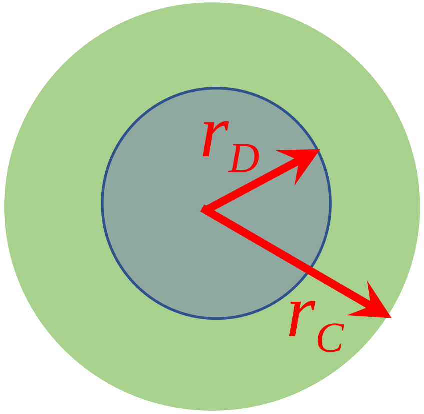

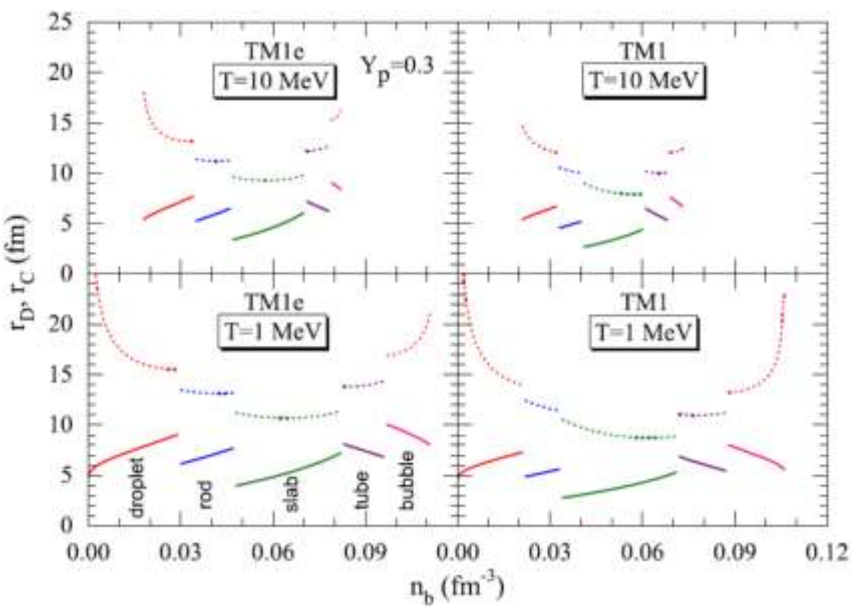

FIG. 3. Size of the nuclear pasta, r_D and that of the Wigner-Seitz cell, r_C as a function of baryon density n_b using the TM1e and TM1 models. The results for Yp = 0.3 at T = 1 and 10 MeV are shown in the lower and upper panels, respectively.

Phase diagrams

* Phase diagrams in the n_b-T plane

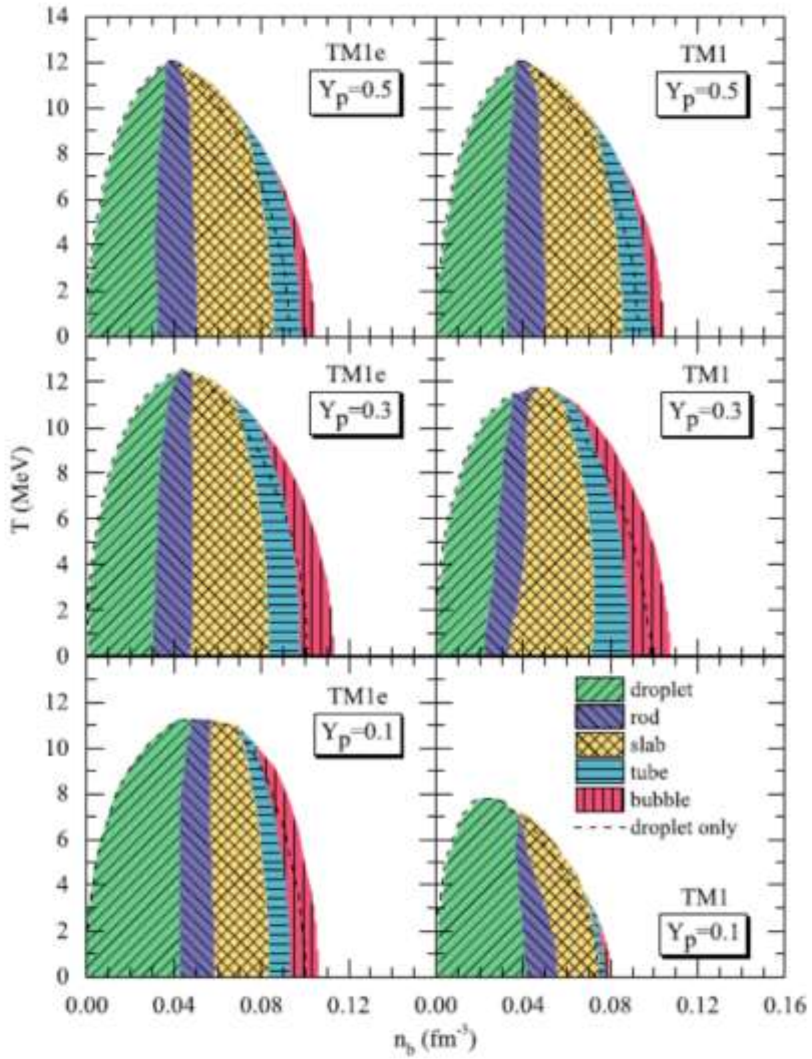

FIG. 1. Phase diagrams in the n_b-T plane for $Y_p = 0.1$, 0.3, and 0.5 obtained using the TM1e and TM1 models. Different colors indicate the regions for different pasta shapes. The boundary of nonuniform matter with only droplet configuration is shown by the dashed line for comparison.

F. Ji, J. N. Hu, S. S. Bao, H. Shen, PRC 102, 015806 (2020)

Phase diagrams

✱ Phase diagrams in the n_b-Y_P plane

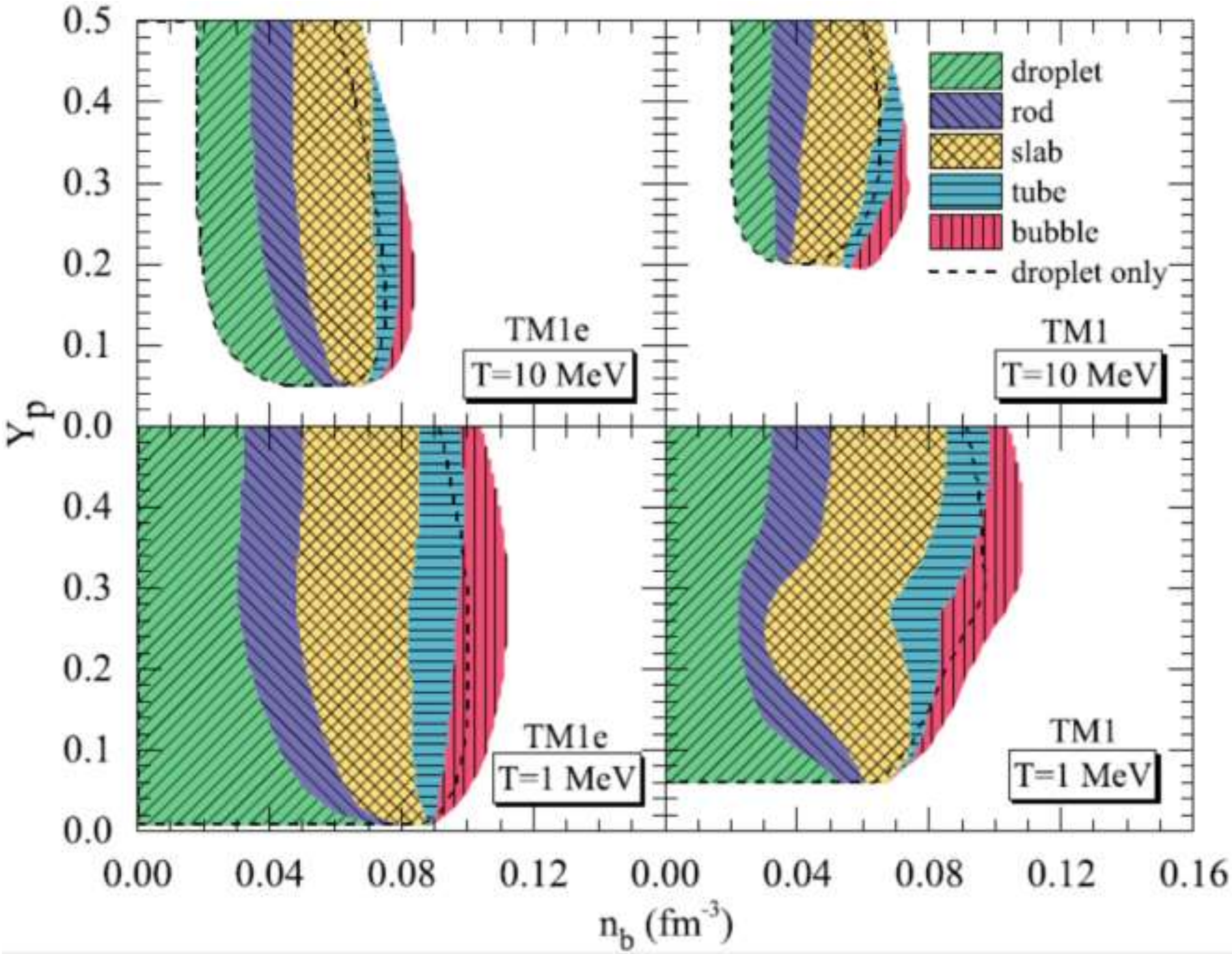

Pasta effect on particle fractions

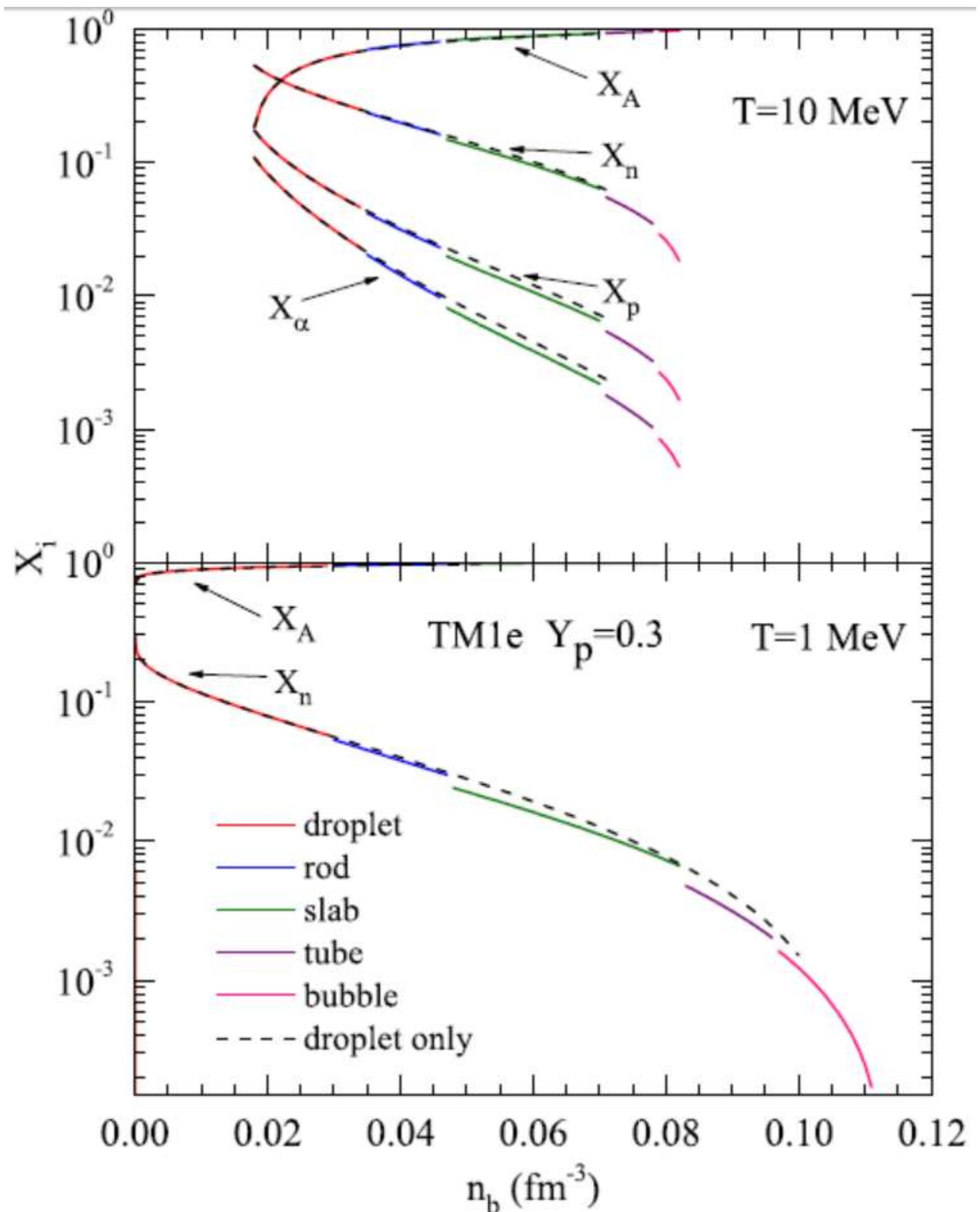

FIG. 6. Fractions of neutrons *(Xn)*, protons (*Xp*), α particles (*Xα*), and heavy nuclei (X_A) as a function of the average baryon density n_b in nonuniform matter for *Yp* = 0.3 at T = 1 and 10 MeV using TM1e.

X_A fraction of nuclei

$$X_A = u\left(n_n^L + n_p^L\right)/n_b$$

X_n X_p fraction of free *n p*

$$X_i = (1-u)\, n_i^G / n_b \quad (i = n, p)$$

X_α fraction of α particles

$$X_\alpha = (1-u)\, 4 n_\alpha^G / n_b$$

Pasta effect on EOS

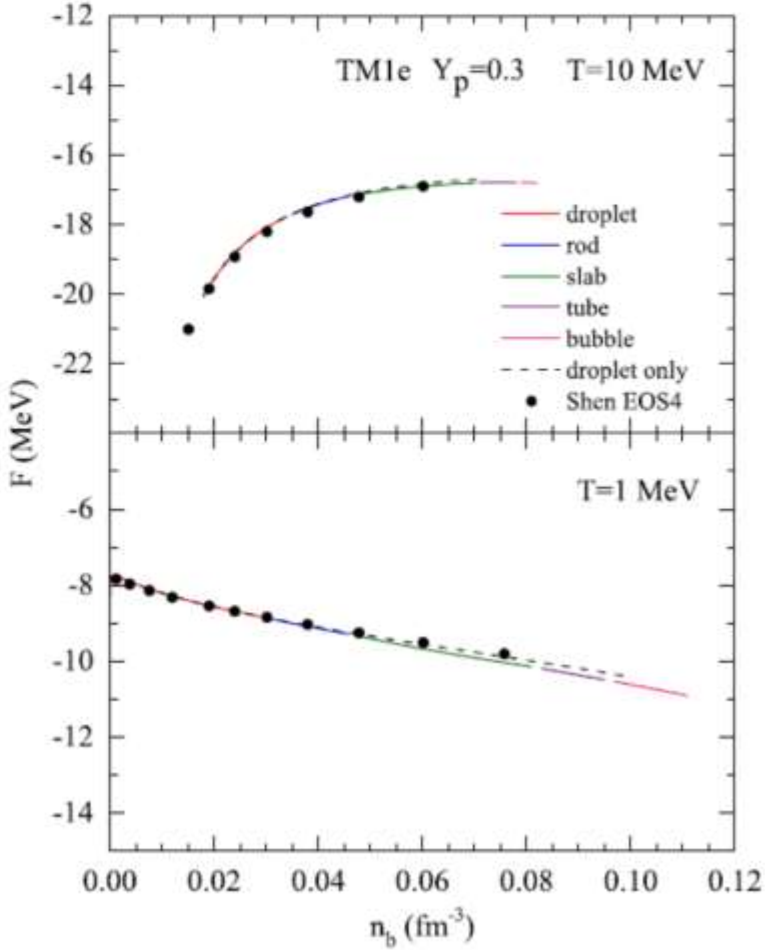

FIG. 7. Free energy per baryon F as a function of n_b for $Yp = 0.3$ at $T = 1$ and 10 MeV using the TM1e

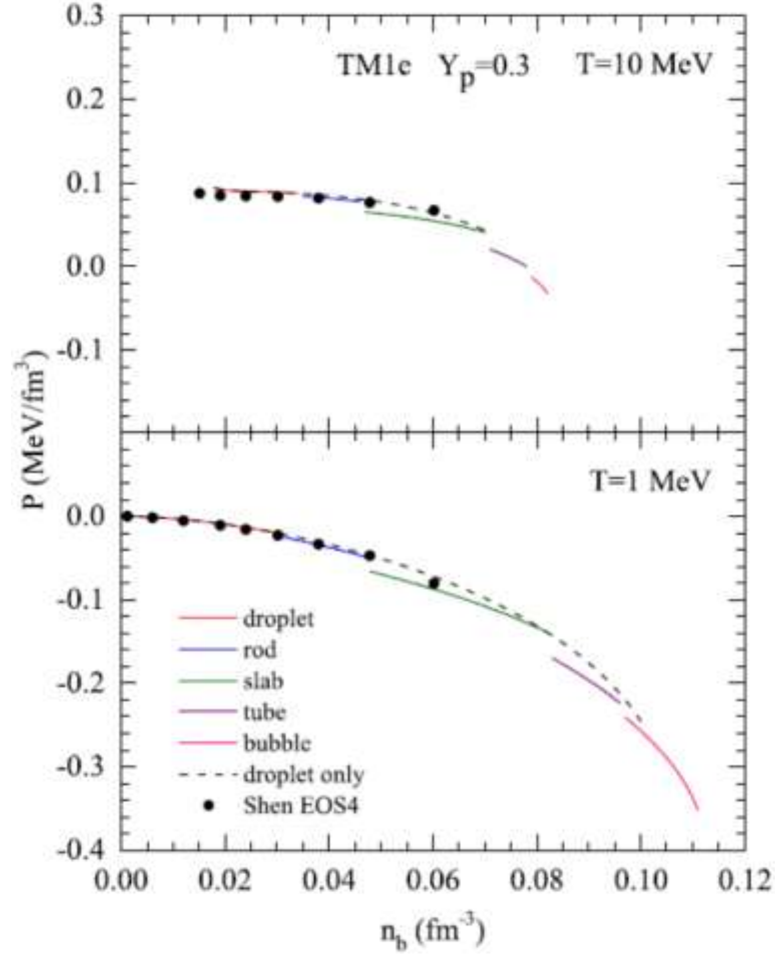

FIG. 8. Same as Fig. 7, but for pressure P

Pasta effect on EOS

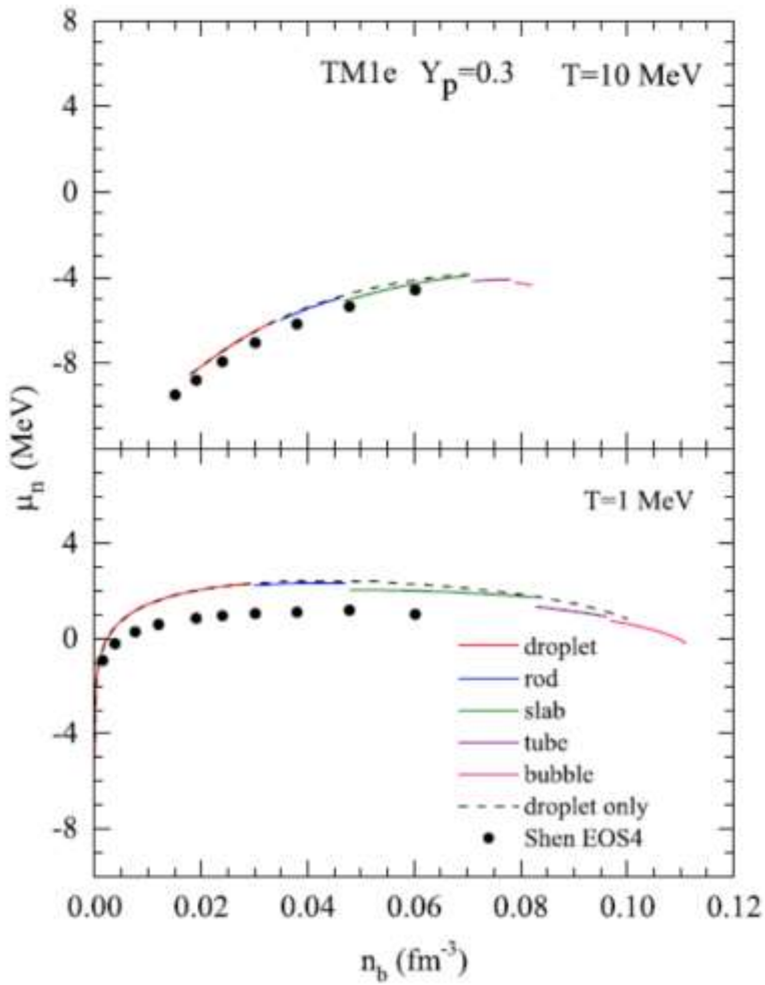

Chemical potential μ_n vs. n_b

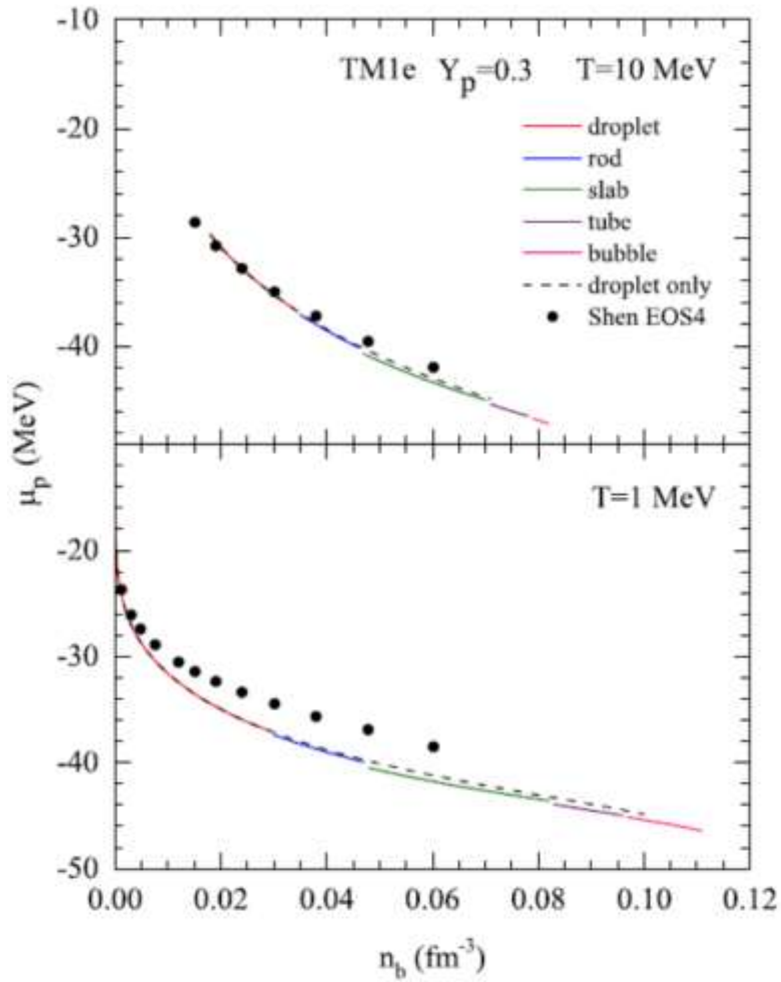

Chemical potential μ_p vs. n_b

Pasta phases in neutron stars

$T = 0$
Y_P by β-equilibrium

outer crust — inner crust — liquid core

$$e+A \rightarrow e+n+A \longrightarrow (e,\mu)+(n,p) \rightarrow + \left\{ \begin{array}{l} \text{hyperons} \\ \text{quarks} \\ \vdots \end{array} \right.$$

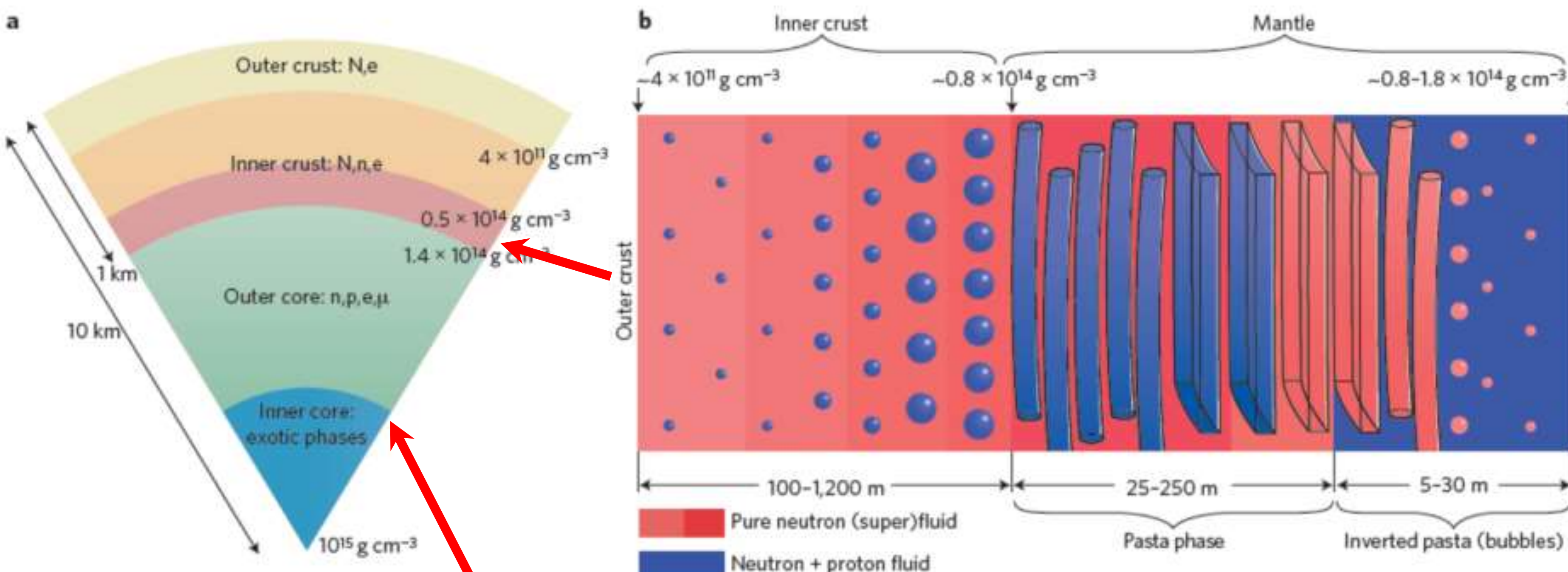

hadron-quark pasta phase

W. G. Newton, Nature Phys. 9 (2013) 396

There are many works by Heiselberg, Maruyama, Tatsumi, Endo, Yasutake, Weber ...

Nuclear pasta phases in inner crust

crust-core transition

* **spinodal instability** (no surface and Coulomb)
  determined by the curvature of the free energy

* **bulk calculation** (no surface and Coulomb)
  phase equilibrium determined by the Gibbs conditions

* **coexisting phases (CP)** (surface and Coulomb perturbatively)
  phase equilibrium determined by the Gibbs conditions

* **compressible liquid-drop (CLD)** (minimization of free energy)
  phase equilibrium determined by minimization

* **Thomas-Fermi (TF)** (realistic description)

Phase diagram of inner crust (TF)

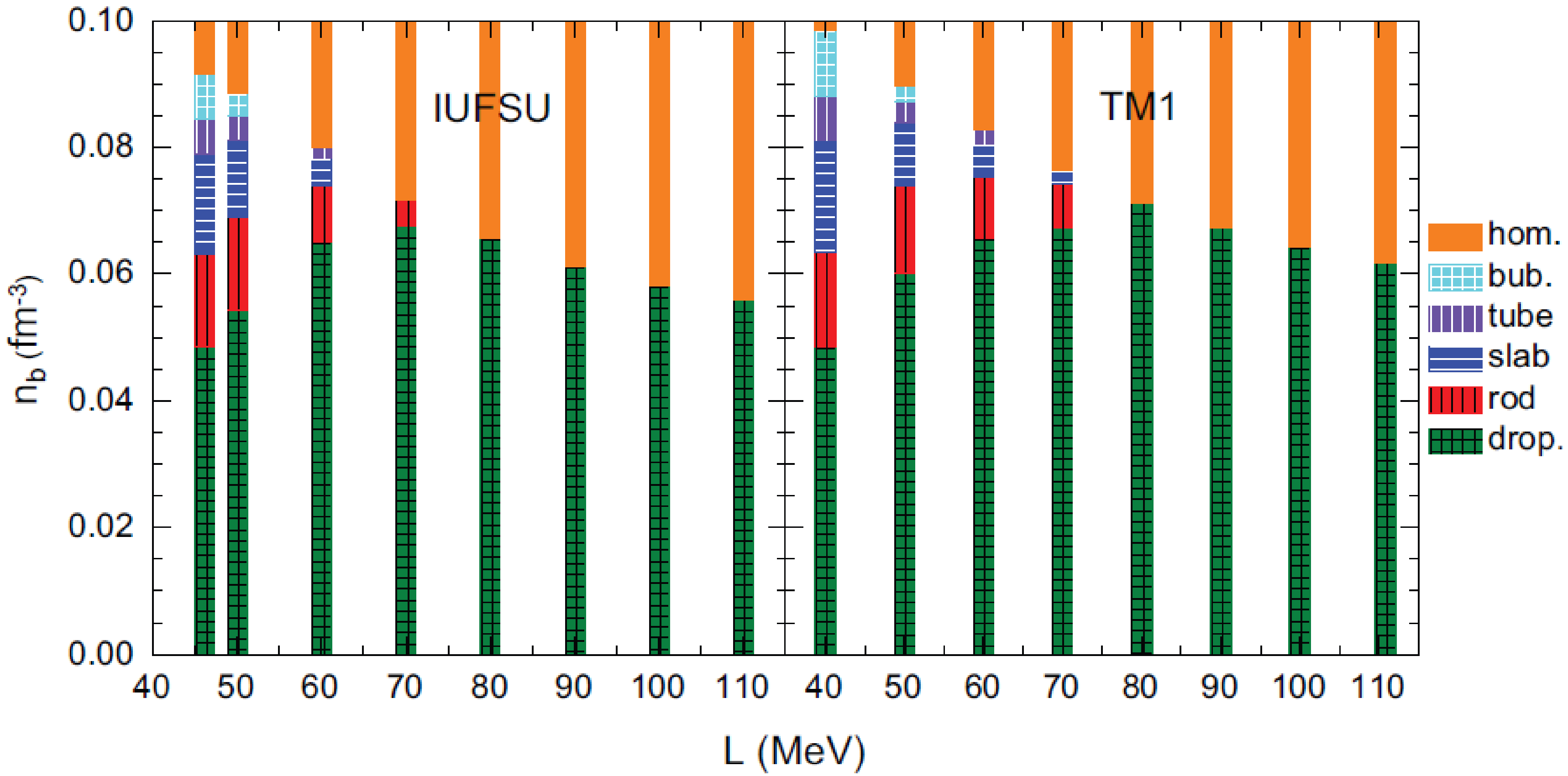

S. S. Bao, H. Shen, Phys. Rev. C 91, 015807 (2015)

smaller L corresponds to more pasta phases

smaller L corresponds to larger crust-core transition density

Distributions of neutrons and protons

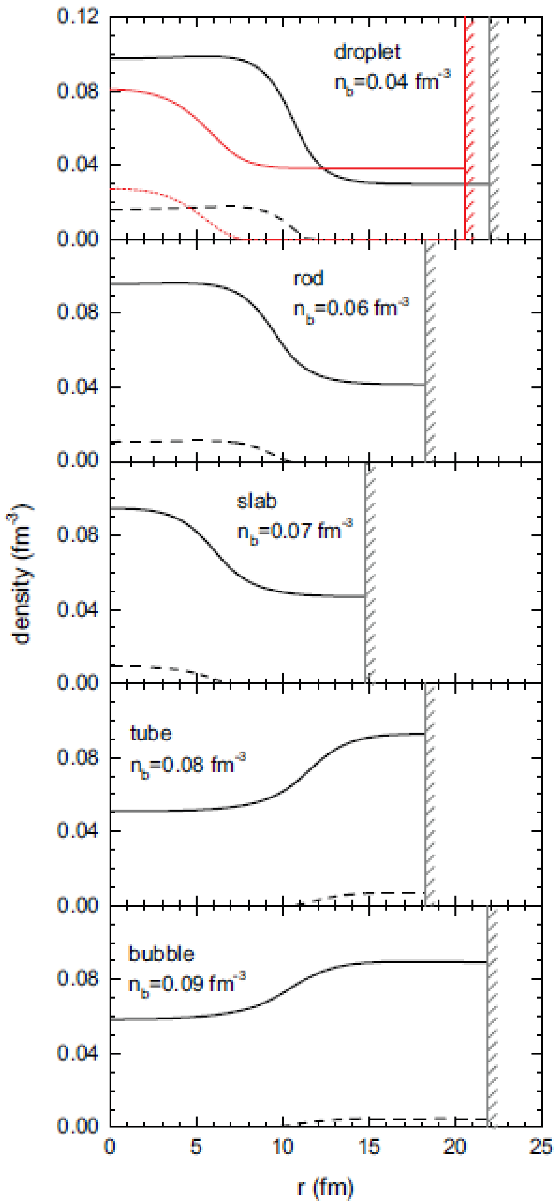

neutron
proton

L=110 MeV

neutron
proton

L=47.2 MeV

self-consistent Thomas-Fermi

S. S. Bao, H. Shen, Phys. Rev. C 91, 015807 (2015)

Hadron-quark pasta phases

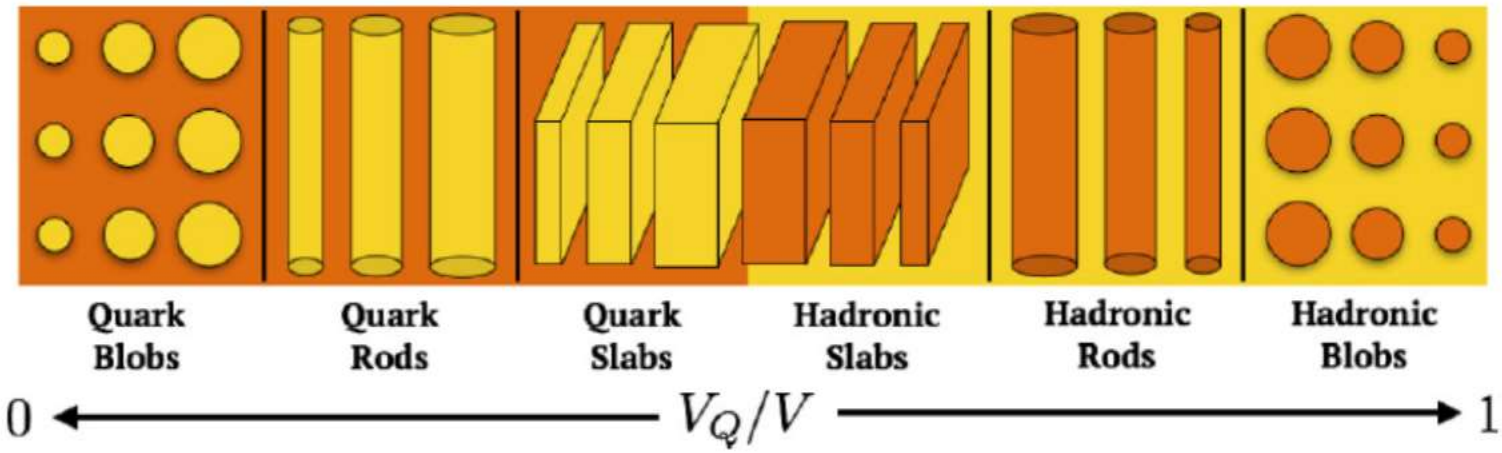

W. M. Spinella, F. Weber, G. A. Contrera, M. G. Orsaria, EPJA 52 (2016) 61

hadronic phase	+	quark phase
Brueckner-Hartree-Fock		MIT bag model
relativistic mean-field		2-flavor NJL model
chiral effective field		3-flavor NJL model
quark-meson coupling		:
:		

Hadron-quark pasta phases

* **Gibbs construction** (no surface and Coulomb)

surface tension: $\sigma = 0 \quad \rightarrow \quad \varepsilon_{\text{surf}} = 2\varepsilon_{\text{Coul}} = 0$

$$\boxed{P_{\text{HP}} = P_{\text{QP}}, \quad \mu_n = \mu_u + 2\mu_d, \quad \mu_e^{\text{HP}} = \mu_e^{\text{QP}}}$$

* **Maxwell construction** (no surface and Coulomb)

surface tension: large σ $\rightarrow$ local charge neutrality $\rightarrow$ $\varepsilon_{\text{surf}} = 2\varepsilon_{\text{Coul}} = 0$

$$\boxed{P_{\text{HP}} = P_{\text{QP}}, \quad \mu_n = \mu_u + 2\mu_d, \quad \mu_e^{\text{HP}} \neq \mu_e^{\text{QP}}}$$

* **coexisting phases (CP)** (surface and Coulomb perturbatively)

phase equilibrium determined by the Gibbs conditions

* **energy minimization (EM)** (surface and Coulomb included in EM)

phase equilibrium determined by energy minimization

Hadron-quark pasta phases

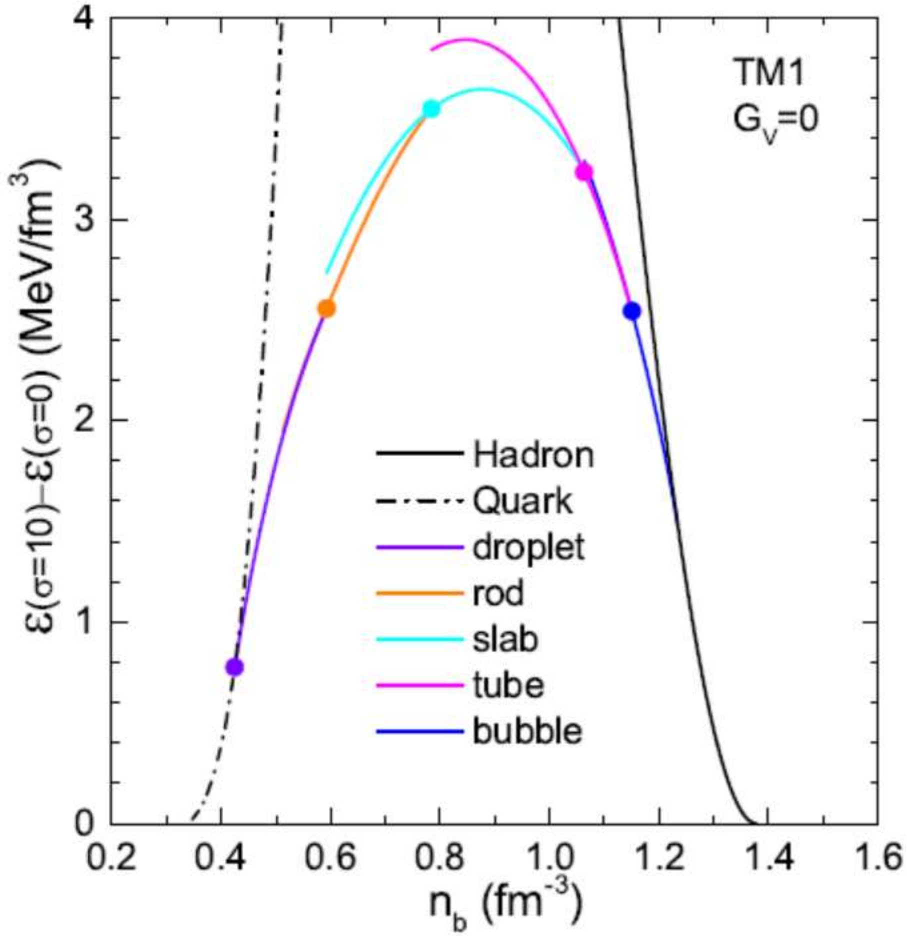

energy densities for pasta phases

hadronic phase

RMF (TM1)

quark phase

NJL (3-flavor)

X. H. Wu, H. Shen, Phys. Rev. C 99, 065802 (2019)

Hadron-quark pasta phases

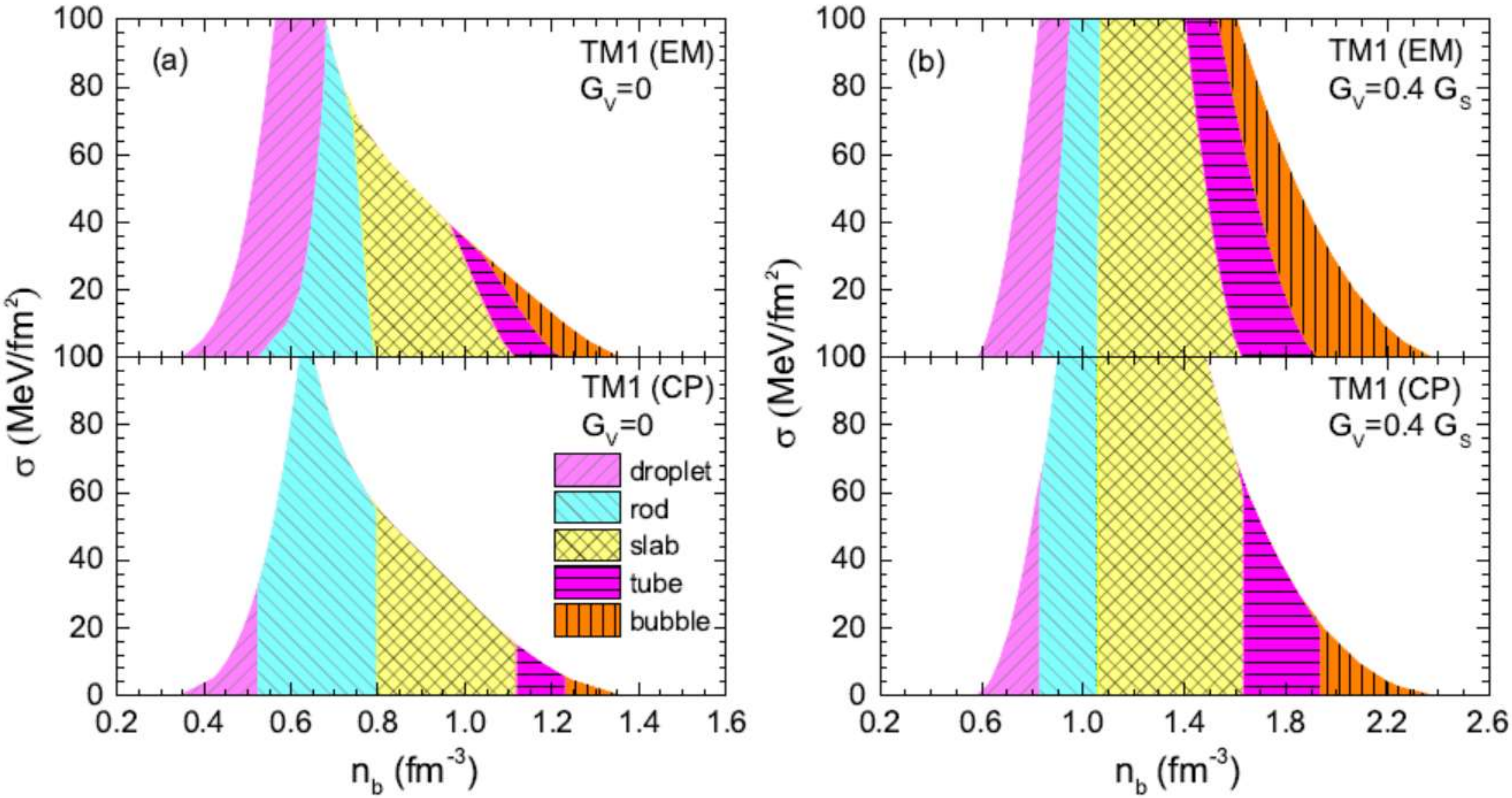

density ranges of pasta phases depend on σ

Surface tension σ

σ obtained in the MIT bag model by using multiple reflection expansion method

$$\sigma_i = \int_0^{k_F^b} \frac{3k_i}{4\pi}\left(1 - \frac{2}{\pi}\arctan\frac{k_i}{m_i}\right)[\mu_i - \sqrt{k_i^2 + m_i^2}]dk_i$$

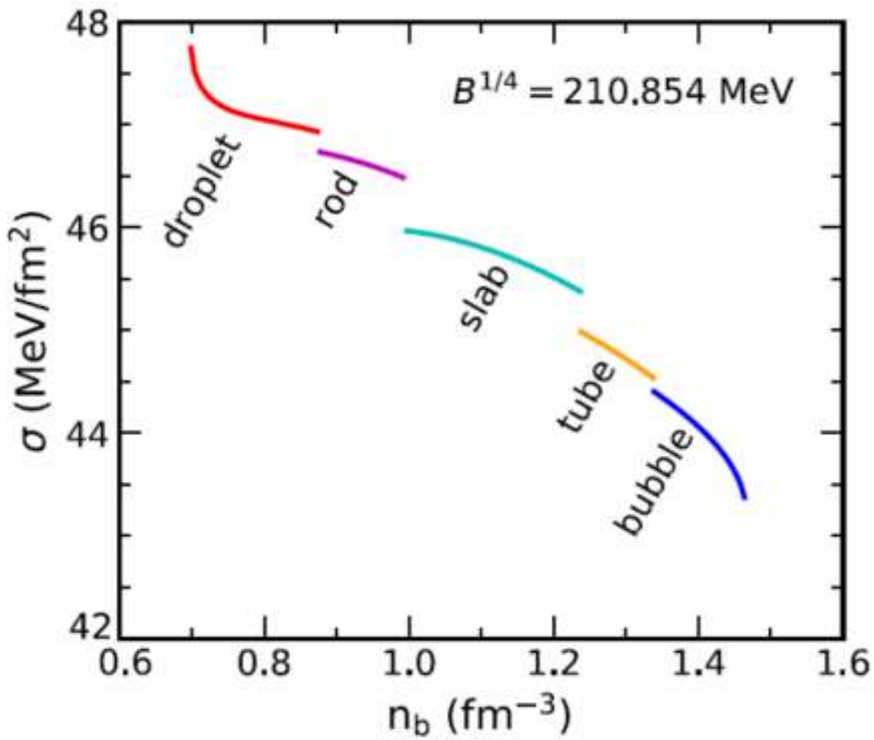

hadronic phase

Quark-Meson-Coupling

(QMC)

quark phase

MIT bag

M. Ju, X.H. Wu, F. Ji, J.N. Hu, H. Shen, Phys. Rev. C 103, 025809 (2021)

Hadron-quark pasta phases

QMC (L = 40)

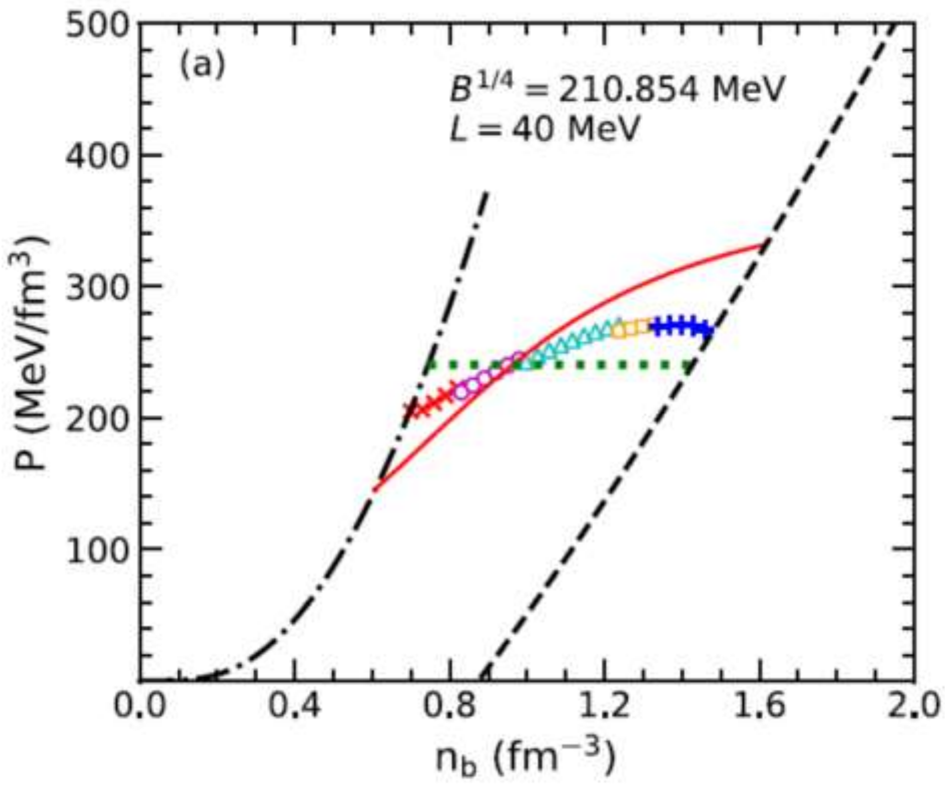

EOS of NS matter

thick lines QMC (L = 40)
thin lines QMC (L = 100)

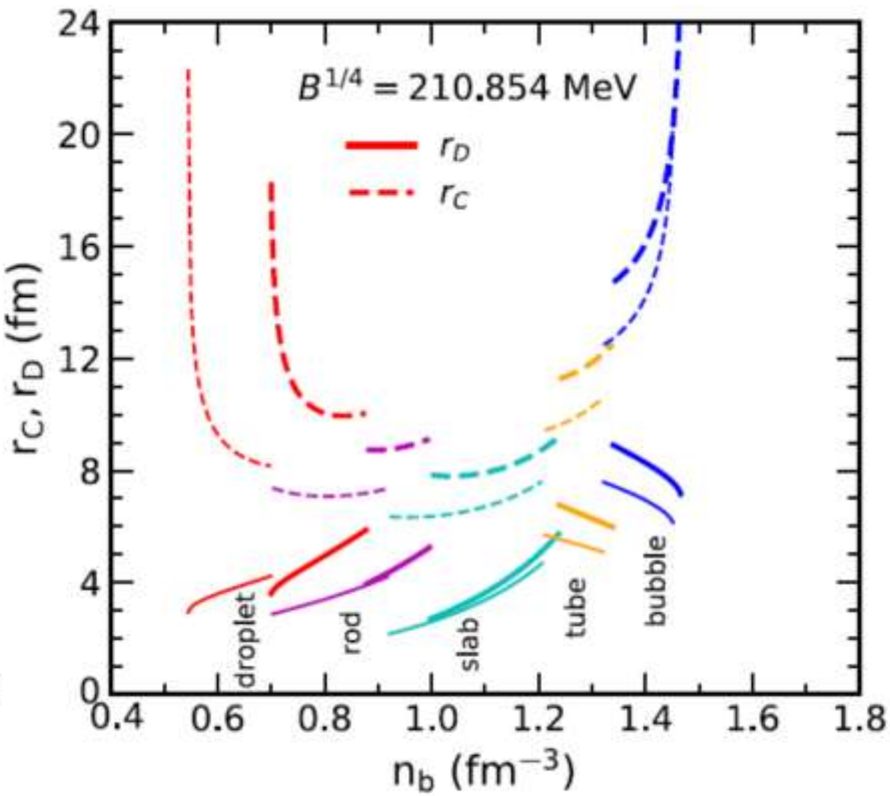

Size of pasta phases

Neutron stars

RMF + vMIT

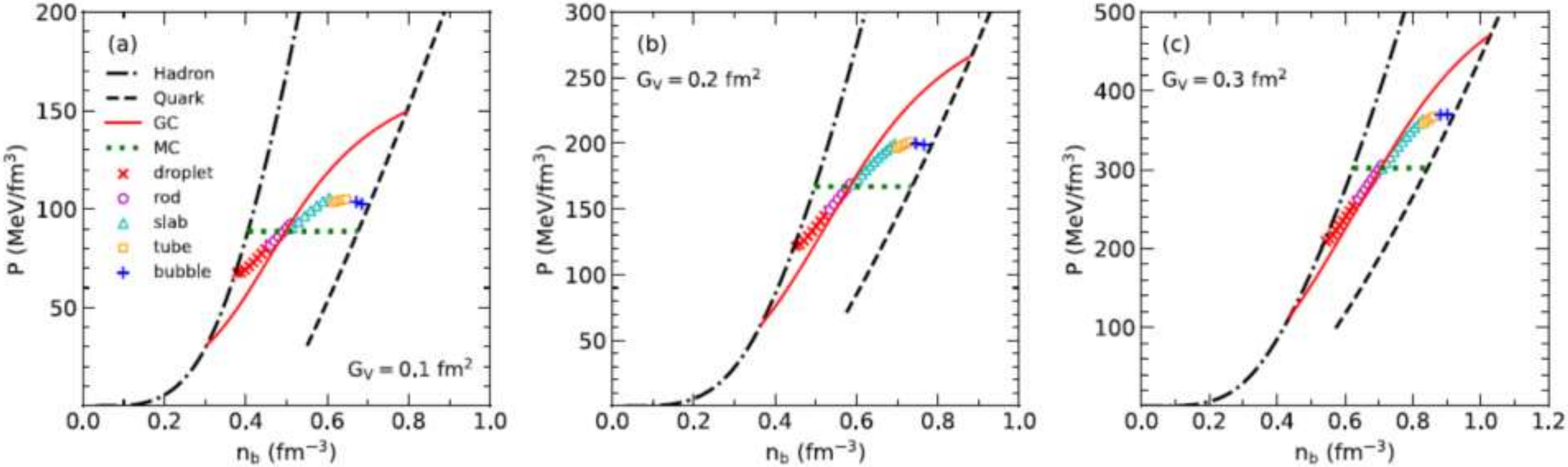

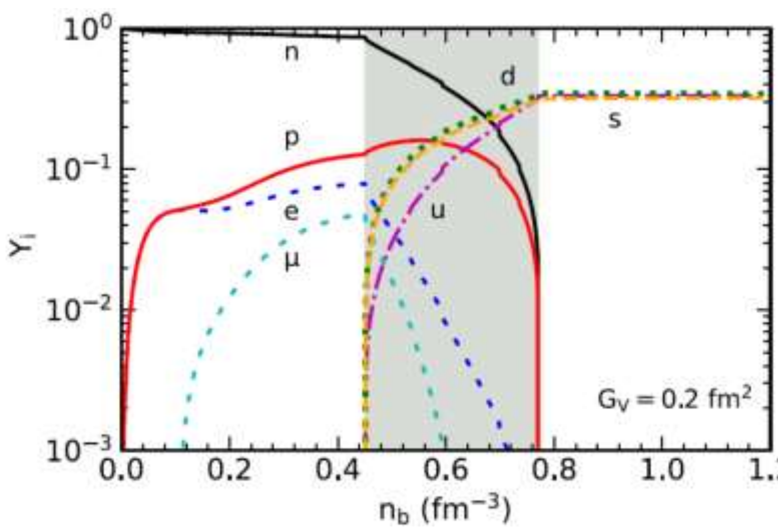

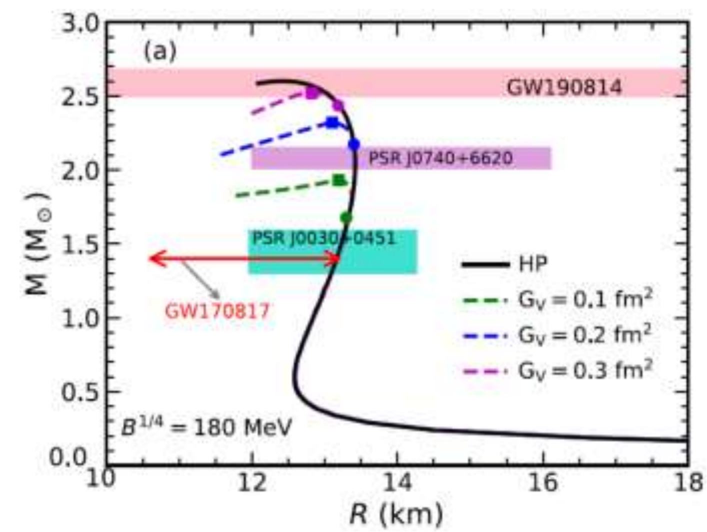

M. Ju, J.N. Hu, H. Shen, Astrophys. J., 923, 250 (2021)

Summary

- Pasta phases can delay the transition to uniform matter
- Pasta phase diagrams depend on L, more clear at low Y_P
- Pasta phases have less influence on E, P, S,...
- Pasta phases in neutron-star crust is sensitive to L
- Hadron-quark pasta phases may exist in neutron-star core